Insulator-metal transition driven by change of doping and spin-orbit interaction in Sr_2IrO_4

J. S. Lee,[1,2,*] Y. Krockenberger,[3] K. S. Takahashi,[3] M. Kawasaki,[1,3] and Y. Tokura[1,3,4]

[1]*Department of Applied Physics and Quantum Phase Electronics Center (QPEC), University of Tokyo, Tokyo 113-8656, Japan*

[2]*Graduate Program of Photonics and Applied Physics, Gwangju Institute of Science and Technology (GIST), Gwangju 500-712, Korea*

[3]*Cross-Correlated Materials Research Group (CMRG) and Correlated Electron Research Group (CERG), ASI, RIKEN, Wako 351-0198, Japan*

[4]*Multiferroics Project, Exploratory Research for Advanced Technology (ERATO), Japan Science and Technology Agency (JST), c/o Department of Applied Physics, University of Tokyo, Tokyo 113-8656, Japan*

(Received 28 November 2011; published 4 January 2012)

We have investigated the insulator-metal transition (IMT) of the 5*d* system Sr_2IrO_4 by optical spectroscopy. Change of the band filling as well as tuning of the spin-orbit interaction (SOI) strength has been realized in single crystalline thin films with continuous cation substitutions. Upon the IMT, the spectral weight of the Mott-gap region is transferred into the in-gap states, and its transfer rate was found to be enhanced similarly to those for the correlated electron system close to the IMT boundary. In particular, the SOI-controlled IMT leads to a characteristic spectral evolution as observed for bandwidth-controlled IMT. The observed feature unambiguously demonstrates the cooperative role of SOI and electron-correlation in realizing the Mott insulator state of Sr_2IrO_4.

DOI: 10.1103/PhysRevB.85.035101 PACS number(s): 78.66.Bz, 71.30.+h, 78.20.Ls, 78.40.Kc

I. INTRODUCTION

Strong electron correlations in transition-metal oxides not only tend to localize conducting electrons but also polarize the electron spins and orbitals. The coupling between the spin and orbital degrees of freedom is triggered by two independent processes, i.e., the entanglement of spin and orbital exchange interactions as described by the Kugel-Khomskii model as well as the relativistic spin-orbit interaction (SOI).[1,2] The latter effect becomes particularly important in compounds containing heavy 5*d* transition metal ions. Comparable energy scales of the Coulomb interaction, the kinetic energy and the SOI promote the competition among electronic orders, realizing electronic and magnetic phases that are not observed for 3*d* and 4*d* transition metal oxides.[3,4] In this context, the layered Sr_2IrO_4 system has attracted great attention since a SOI-induced Mott-insulator state is established; the $J_{\rm eff} = 3/2$ state is fully occupied, and the $J_{\rm eff} = 1/2$ state is half filled and splits to form the Mott-Hubbard bands due to electronic correlations.[3–7] A phase diagram with various competing electronic phases is expected in the vicinity of such a SOI-induced Mott insulator,[7,8] though high-quality samples remained elusive. Experimental progress on the metallic state in iridates, e.g., $Sr_2IrO_{4-\delta}$ ($\delta \leqslant 0.04$)[9] and $SrIrO_3$,[10] have been reported.

In general, the control of physical properties by cation substitution may be performed with superior precision. In Fig. 1, we introduce changes in three important electronic parameters, i.e., band filling, electron correlation effect, and the SOI strength ($\lambda_{S\text{-}O}$) with respect to those for Sr_2IrO_4 upon the cation substitutions. The substitution of divalent Sr by trivalent La in $Sr_{2-y}La_yIrO_4$ tunes the band filling (electron doping). An isoelectronic substitution of Ir with Rh in $Sr_2Ir_{1-x}Rh_xO_4$ reduces $\lambda_{S\text{-}O}$ in the virtual crystal (amalgamated-band) scheme since $\lambda_{S\text{-}O}$ is significantly weaker in 4*d* elements, albeit with the anticipated slight increase in the electron correlation as represented by *U*/*W*, where *U* is the on-site Coulomb repulsion energy and *W* is the one-electron bandwidth. A substitution of Ir with Ru in $Sr_2Ir_{1-x}Ru_xO_4$ simultaneously tunes the band filling (hole doping) as well as $\lambda_{S\text{-}O}$. In this case, the *U*/*W* may increase or decrease depending on the relative contribution of the less structural distortion[11] and the less extended 4*d* orbitals for Sr_2RuO_4, which will increase *W* and *U*, respectively.

While there have been several investigations on the transport and magnetic properties for $Sr_{2-y}La_yIrO_4$,[12–14] $Sr_2Ir_{1-x}Rh_xO_4$,[12,13] and $Sr_2Ir_{1-x}Ru_xO_4$,[15,16] all of them have used polycrystalline samples. Considering the layered crystal structure of these systems, however, single crystalline samples are indispensable to address their anisotropic properties more properly. In this paper, we have prepared epitaxial single-crystalline thin films of aforementioned materials and investigated in-plane optical conductivity spectra upon the

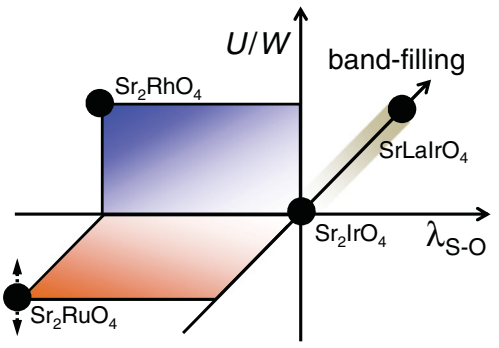

FIG. 1. (Color online) Schematic diagram showing changes in band filling, electron correlation effect, and the SOI strength $\lambda_{S\text{-}O}$ with respect to those for Sr_2IrO_4 upon the cation substitutions. Here, electron correlation is represented by the ratio between the on-site Coulomb repulsion energy *U* and the conduction bandwidth *W*. For $La_ySr_{2-y}IrO_4$, the electron-doping is achieved with the other two parameters unchanged. For $Sr_2Ir_{1-x}Rh_xO_4$, *U*/*W* is expected to increase and $\lambda_{S\text{-}O}$ to decrease while the band filling is preserved. For $Sr_2Ir_{1-x}Ru_xO_4$, all the three parameters are expected to change as indicated. For *U*/*W*, it is not straightforward to declare whether it increases or decreases with the Ru substitution.

insulator-metal transition. Since the optical conductivity is sensitive not only to the electric properties but also to the $J_{\rm eff}$ states,[4] they can provide us with important information about the electronic structural evolutions upon the insulator-metal transition driven by electron/hole doping and/or SOI tuning.

II. EXPERIMENTAL

Single-crystalline films of $Sr_{2-y}La_yIrO_4$ ($y = 0.1$ and 0.2) were grown on (001)$SrTiO_3$ substrates by pulsed laser deposition. Hall effect measurements indicate that the charge carriers are electron-like for these compounds, as expected, whereas they are holelike for undoped Sr_2IrO_4.[17] Composition-spread films of $Sr_2Ir_{1-x}Rh_xO_4$ ($0 < x < 0.5$) and $Sr_2Ir_{1-x}Ru_xO_4$ ($0 < x < 1.0$) were grown on $(001)(LaAlO_3)_{0.3}(SrAl_{0.5}Ta_{0.5}O_3)_{0.7}$ (LSAT) substrates. The chemical composition at each sample position was characterized with a scanning electron microscope (SEM) equipped with an energy dispersive x-ray (EDX) spectrometer, and the results are shown in Figs. 2(a) and 2(b).[18] The composition (x) varies continuously along the lateral direction of the substrate over several millimeters.[18,19] Figures 2(c) and 2(d) show intensity distribution of x-ray diffraction related to the lattice constant along the surface normal direction at room temperature, which is obtained from concurrent $2\theta/\theta$ x-ray diffraction for the (002) Bragg peak from the substrate and (006) peak from the film. They confirm a continuous variation of the c-axis length with the cation substitutions. Note that the (006) Bragg peak for $Sr_2Ir_{1-x}Rh_xO_4$ becomes diffusive as the lateral distance is larger than 4 mm. This indicates the sample crystallinity is not good for the Rh content larger than about 0.5 [see Fig. 2(b)].

Reflectivity spectra (R) of the infrared and near-infrared/visible region have been taken by Fourier-transformation- and grating-type spectrometers, respectively.

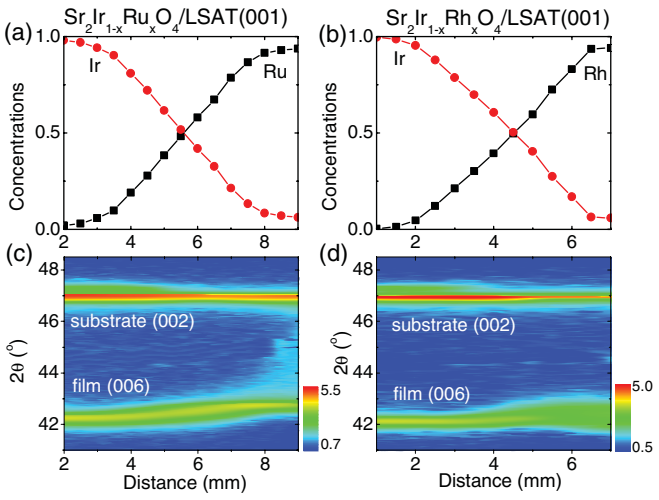

FIG. 2. (Color online) (a) and (b) The concentrations of transition metal ions as a function of the lateral distance in composition-spread films of $Sr_2Ir_{1-x}Ru_xO_4$ and $Sr_2Ir_{1-x}Rh_xO_4$. (c) and (d) Intensity distribution of the x-ray diffraction related to the lattice constant along the surface normal direction at room temperature. It is obtained from concurrent $2\theta/\theta$ x-ray diffraction for the (002) Bragg peak and (006) Bragg peak from the substrate and the film, respectively.

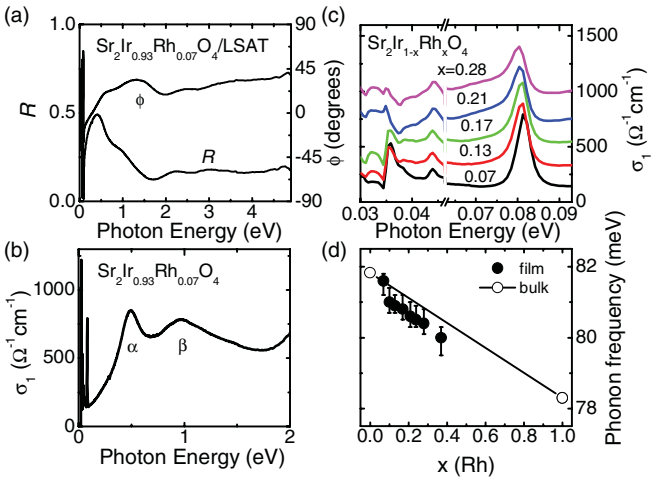

FIG. 3. (Color online) The optical responses of $Sr_2Ir_{1-x}Rh_xO_4$ grown on (001)LSAT substrate. (a) The reflectivity spectrum (R) for $x = 0.07$ and the corresponding phase factor (ϕ) obtained through the Kramers-Kronig transformation of the reflectivity. (b) Real part of the optical conductivity spectrum of the film. (c) The optical conductivity spectrum in the far-infrared region. (d) The frequency of the Ir/Rh-O stretch mode as a function of the Rh content x. The values for the bulk end members are also included as open symbols.[21,25]

In particular, our custom designed scanning microscope allows a typical spatial resolution of 100–200 μm for the investigation of composition-spread thin films.[18] The phase change (ϕ) upon the reflection was determined via Kramers-Kronig transformation as shown in Fig. 3(a). The optical constants of the thin films were numerically evaluated, where the substrate contributions to the reflection process have been subtracted.[20] Figure 3(b) exemplifies the real part of the optical conductivity spectra $\sigma_1(\omega)$ for $x = 0.07$ of $Sr_2Ir_{1-x}Rh_xO_4$. Two peaks are observed around 0.5 eV and 1.0 eV, and they are assigned to the optical excitations from the $J_{\rm eff} = 1/2$ and 3/2 occupied states to the unoccupied $J_{\rm eff} = 1/2$ (upper Hubbard band) state,[10,21,22] respectively. Hereafter, we term these excitations α and β, respectively, in accord with literature.[4] $\sigma_1(\omega)$ in the far-infrared region for representative samples are shown in Fig. 3(c) where three phonon modes are observed around 35, 45, and 80 meV in the low-x compounds. The stretching mode of the Ir/Rh-O bond,[21,23,24] located at the highest energy, shows a systematic change of its energetic position upon Rh substitution x [see Fig. 3(d)].[21,25] A linear interpolation between the two end-member compounds supports the view of the formation of a solid solution of Ir and Rh.

III. RESULTS AND DISCUSSIONS

Figure 4 shows $\sigma_1(\omega)$ for $Sr_{2-y}La_yIrO_4$, $Sr_2Ir_{1-x}Rh_xO_4$, and $Sr_2Ir_{1-x}Ru_xO_4$ obtained at room temperature. While two excitations are clearly observed around 0.5 and 1 eV for the compounds close to Sr_2IrO_4, the conductivity in the lower-energy region increases with an increase of y or x, indicating the transition to the metallic state. For instance, the conductivity level in the far-infrared region exceeds 1000 $\Omega^{-1}{\rm cm}^{-1}$ for $x = 0.28$ of $Sr_2Ir_{1-x}Rh_xO_4$ [see also Fig. 3(c)]. Nevertheless, the low-energy excitation does not show a Drude-like response, indicating that the conduction remains in an incoherent regime

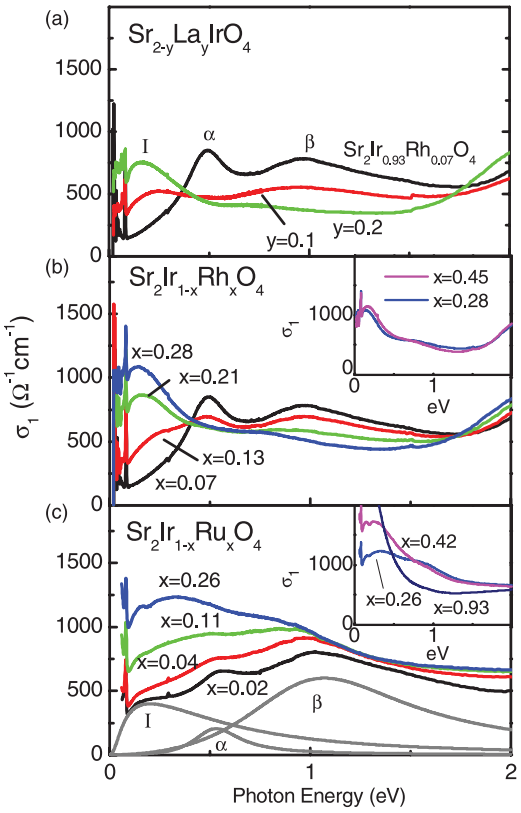

FIG. 4. (Color online) Optical conductivity spectra $\sigma_1(\omega)$ for $La_ySr_{2-y}IrO_4$ (a), $Sr_2Ir_{1-x}Rh_xO_4$ (b), and $Sr_2Ir_{1-x}Ru_xO_4$ (c) obtained at room temperature for various substitution levels. The insets for (b) and (c) show spectra with high x values. Gray curves in (c) are fitting curves for the peak I, α, and β for $x = 0.02$.

at the early stage of the insulator-metal transition.[26,27] For $Sr_{2-y}La_yIrO_4$ and $Sr_2Ir_{1-x}Rh_xO_4$, the spectral weight in the low-energy region appears to be transferred from the gap transition region above 0.4 eV, forming a well defined isosbestic point (equal-absorption point). Such a spectral weight transfer from the Mott gap region to the inner-gap one coincides with the feature typically observed in Mott-transition systems.[27–30] For $Sr_2Ir_{1-x}Ru_xO_4$, on the other hand, the optical conductivity increases over the full spectral region below 2 eV as x increases up to $x \simeq 0.5$.

To get a more insight to the spectral changes, it is useful to fit the optical conductivity spectra by using Lorentz oscillators,

$$\sigma_1(\omega) = \frac{1}{4\pi} \sum_i \frac{S_i \omega^2 \Gamma}{\left(\omega_i^2 - \omega^2\right)^2 + \Gamma^2 \omega^2}, \qquad (1)$$

where S_i, ω_i, and Γ_i are strength, energy, and damping factor of ith oscillator. Figures 4(c) and 6(a) show examples of the fitting results for $x = 0.02$ of $Sr_2Ir_{1-x}Ru_xO_4$ and $x = 0.07$ of $Sr_2Ir_{1-x}Rh_xO_4$, respectively, where the three conductivity curves correspond to the inner-gap excitation I, peak α, and peak β. The effective number of electrons N_{eff} of the ith oscillator is estimated by its definition $N_{\text{eff}} = \frac{m}{4\pi Ne^2} S_i$. Here, m is the free electron mass and N the number of transition metal ions (Ir, Ru, or Rh) per unit volume that was simply referred to the values of bulk Sr_2IrO_4 samples.[31] For $Sr_2Ir_{1-x}Ru_xO_4$, more than one peak are required to fit the spectra below 0.5 eV, thus we accumulated the sum of all the excitations located below the peak α as the inner-gap excitation I.

In Fig. 5(a), we present ΣN_{eff}, the summation of N_{eff} of the inner-gap excitation I, peak α, and peak β. It is interesting to note that ΣN_{eff} remains almost constant for $Sr_2Ir_{1-x}Rh_xO_4$, in agreement with our assumption of the constant band filling. With an isoelectronic Rh substitution, the band filling of the d-electron states remains unchanged as d^5, and consequently the density product of the occupied and unoccupied states within the t_{2g} manifold should be constant, if the electronic bands are well amalgamated in the mixed crystals. On the other hand, ΣN_{eff} changes differently in the other compounds; ΣN_{eff} decreases slightly with the La substitution, and it increases strongly with the Ru substitution. While the changes in the band filling would be responsible for such behaviors, there should be more effects to be considered for the Ru substitution that will agitate the d-electron system more strongly (see Fig. 1) through the change in structural distortions and possible large difference in p-d electron hybridization.[11]

The N_{eff} of the inner-gap excitation (I) shows qualitatively similar behaviors with the chemical substitution procedures for all the three composition-controlled materials series; as shown in Fig. 5(b),[32] it increases monotonously with x or y, indicating the increase of the kinetic energy of conduction electrons. Interestingly, N_{eff} for the Ru-doping increases significantly faster than the other two cases. This may be first understood by the add-up of two effects, i.e., the carrier doping and

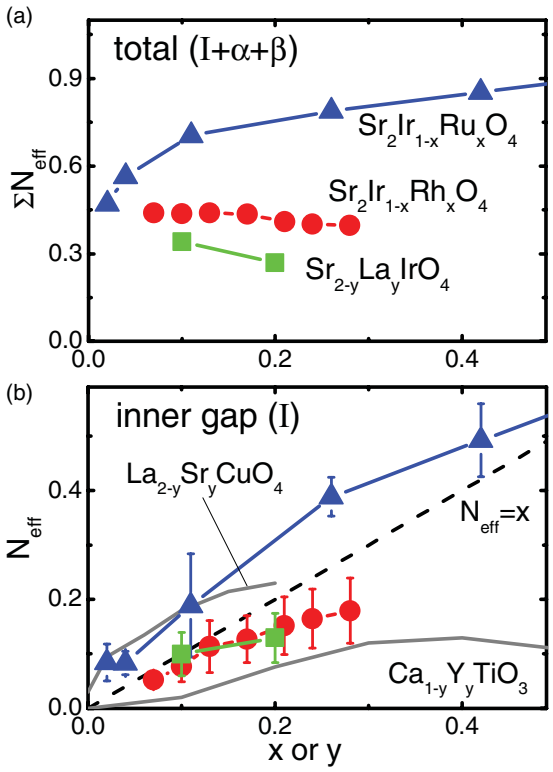

FIG. 5. (Color online) Evolution of the spectral weight (N_{eff}, see text for definition) with chemical substitution (x or y) in $La_ySr_{2-y}IrO_4$, $Sr_2Ir_{1-x}Rh_xO_4$, and $Sr_2Ir_{1-x}Ru_xO_4$. (a) The summation of N_{eff} of the inner-gap excitation I, peak α, and peak β. (b) N_{eff} of the inner-gap excitation only. The corresponding values for $La_{2-y}Sr_yCuO_4$[28] and $Ca_{1-y}Y_yTiO_3$[29] are also shown.

the SOI reduction, which turned out, respectively, to have similar amount of the contribution to the low-energy spectral weight as observed for the La- and Rh-doping, respectively. Additionally, the strong hybridization between the transition metal d and O $2p$ orbital in the Sr_2RuO_4 side with a higher (tetragonal) structural symmetry may also contribute to the enhancement of the low-energy spectral weight.[11]

A comparison to other quantum spin ($S = 1/2$ or $J_{\rm eff} = 1/2$) Mott transition systems provides valuable information on the influence of the band-filling change in Sr_2IrO_4. As representative cases, $N_{\rm eff}$ of layered cuprates $La_{2-y}Sr_yCuO_4$ and distorted-perovskite $Ca_{1-y}Y_yTiO_3$ are displayed.[28,29] Note that there are several other compounds showing $N_{\rm eff}$ in between, such as $Ca_{1-y}La_yTiO_3$ and $Sr_{1-y}La_yTiO_3$.[33,34] Katsufuji *et al.* have demonstrated that the rate of the low-energy part (or inner-gap excitation) evolution with the doping level is critically enhanced as the electron correlation strength approaches the critical value of the bandwidth-controlled Mott transition.[34] In this context, the enhanced rate of $N_{\rm eff}$ for $Sr_{2-y}La_yIrO_4$ and $Sr_2Ir_{1-x}Ru_xO_4$ in the present case demonstrates that Sr_2IrO_4 locates on the verge of the phase transition to the metallic state.[6] Hence electron- as well as hole-doping provides an effective route to increase the kinetic energy of the conduction electrons.

In the following, the observed variations of gap excitations α and β are discussed. Since these two excitations are assignable to the transitions from the occupied $J_{\rm eff} = 1/2$ (lower Hubbard band) and $J_{\rm eff} = 3/2$ state to the unoccupied $J_{\rm eff} = 1/2$ (upper Hubbard band) state, respectively, the change of these excitations can reveal how the SOI-induced $J_{\rm eff}$ states evolve upon the insulator-metal transitions. For $La_{2-y}Sr_yIrO_4$, the La substitution leads to the disappearance of the peak α accompanied by the closing of the optical gap (see Fig. 4). This should be understood by the formation of the doping-induced in-gap state as usually observed in $3d$ transition metal oxides with filling control.[27–30,34] For $Sr_2Ir_{1-x}Ru_xO_4$, the hole doping with Ru substitutions, among several possible effects, will affect the band structure similarly

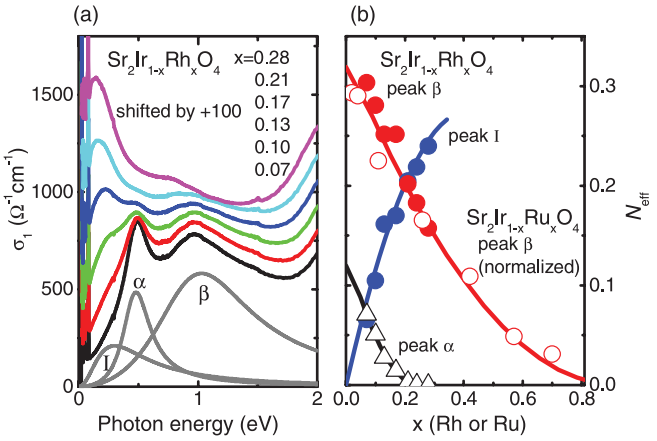

FIG. 6. (Color online) (a) $\sigma_1(\omega)$ for $x = 0.07$–0.28 of $Sr_2Ir_{1-x}Rh_xO_4$. The curves are shifted upward for clarity. Gray lines are fitting curves with the peak I, α, and β for $x = 0.07$. (b) $N_{\rm eff}$ for the peaks I, α, and β. Also shown is $N_{\rm eff}$ of the peak β for $Sr_2Ir_{1-x}Ru_xO_4$, which is normalized by the sum of $N_{\rm eff}$ of the peak I, α, and β. The solid lines are guides to the eye.

to induce the in-gap state close to the Fermi level. The schematic diagram of the electronic structures for these cases are depicted in Fig. 7 where the end members of $SrLaIrO_4$ and Sr_2RuO_4 are assumed to be a band insulator and a band metal, respectively.

While the Rh substitution gives rise to the similar spectral changes related to the peak α and the lower energy excitation, the driving mechanism should be understood differently since the band filling is preserved in the amalgamated $4d$-$5d$ band scheme in this case. Figure 6(a) shows $\sigma_1(\omega)$ of $Sr_2Ir_{1-x}Rh_xO_4$, where the spectra are arbitrarily shifted upward with x to visualize the peak structures. As x increases, the optical gap is closed while peak I develops and gradually shifts to the lower energies. The collapse of the Mott gap is accompanied by the suppression of the peak α (as well as the peak β), while the spectra for $0.13 \leqslant x \leqslant 0.21$ clearly show the coexistence of the inner-gap excitation and the peak α. It should be noted that such a clear distinction of the low-energy peaks were not observed for $La_{2-y}Sr_yIrO_4$ (and $Sr_2Ir_{1-x}Ru_xO_4$ as well). Compared to the in-gap state arising from the electron or hole doping, this suggests that a new state emerging from the Rh substitution should be located further away from both the Hubbard bands. This behavior is reminiscent of quasiparticle peak formed between the Mott-Hubbard bands during the bandwidth-controlled metal-insulator,[27,30] as shown in the middle panel of Fig. 7(b). It is worth to note that such a correlated metallic state for $Sr_2Ir_{1-x}Rh_xO_4$ emerges from the Mott insulator state driven by the dominating effect of decreasing SOI over the slight enhancement of electron correlation.[35]

A further increase of x leads to the complete suppression of the peak α. Notwithstanding, the peak β survives even up to about $x = 0.45$ as shown in the inset of Fig. 4(b). Such

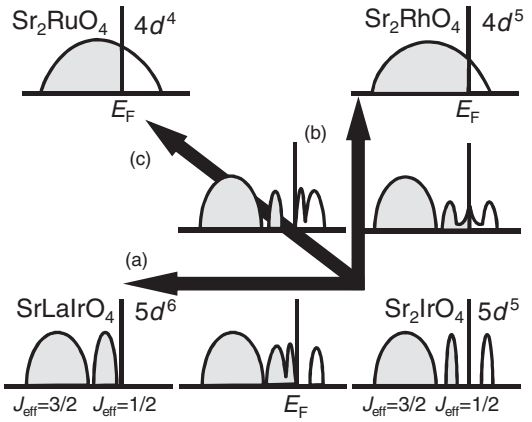

FIG. 7. Schematic diagram of the electronic states near the Fermi level (E_F) for $La_ySr_{2-y}IrO_4$ (a), $Sr_2Ir_{1-x}Rh_xO_4$ (b), and $Sr_2Ir_{1-x}Ru_xO_4$ (c). Vertical lines correspond to the E_F. Sr_2RuO_4 and Sr_2RhO_4 are considered as a simple band metals. For Sr_2IrO_4, $J_{\rm eff}$ states are arranged to induce the Mott gap in the half-filled $J_{\rm eff} = 1/2$ state whereas the other $J_{\rm eff} = 3/2$ state is fully occupied. $SrLaIrO_4$ is assumed to have a similar electronic structure to Sr_2IrO_4, though the band filling is altered. Electron- or hole-doping seeds in-gap states below or above E_F, which is shown in the center of (a) and (c). The reduction of the spin-orbit interaction allows the development of the quasiparticle peak at E_F as shown in the middle of (b).

behaviors can be seen more clearly in Fig. 6(b) where $N_{\rm eff}$ values for these excitations are displayed as a function of x. The results indicate that the Hubbard splitting of the $J_{\rm eff} = 1/2$ band readily collapses for reduced SOI values, whereas the $J_{\rm eff} = 1/2$ and $3/2$ states themselves remain robust while keeping similar energy splitting of about 0.5 eV. In Fig. 6(b), $N_{\rm eff}$ of the peak β for $Sr_2Ir_{1-x}Ru_xO_4$ (hole-doping case) is shown after being normalized by multiplying $\Sigma N_{\rm eff}(x = 0)/\Sigma N_{\rm eff}(x)$ with $\Sigma N_{\rm eff}(x = 0) \simeq 0.43$ to account for the hole-doping effect. Interestingly, a nearly parallel behavior for $Sr_2Ir_{1-x}Ru_xO_4$ is observed, thus indicating that the Rh or Ru substitutions have a similar influence on the electronic structure with respect to the SOI.

IV. SUMMARY

We have investigated the insulator-to-metal transition (IMT) of the $5d$ system Sr_2IrO_4. The roles of the band filling and/or the spin-orbit interaction (SOI) have been examined by optical spectroscopy of high-quality, single-phase thin films of $Sr_{2-y}La_yIrO_4$ and composition-spread thin films of $Sr_2Ir_{1-x}Rh_xO_4$ and $Sr_2Ir_{1-x}Ru_xO_4$. Clearly, the Mott gap collapses upon chemical substitutions, and the spectral weight above the gap rapidly transfers to the inner gap excitations. This shift of spectral weight manifests the contiguity of the SOI-induced Mott insulating state of Sr_2IrO_4 to the metal-insulator phase boundary. Furthermore, as is the case for band-width controlled IMT, the reduction of the SOI leads to comparable spectral weight evolutions. This observation confirms the picture that the electron correlation and the SOI are cooperatively influencing the Mott insulator state in Sr_2IrO_4. We emphasize that apart from the fragility of the Mott gap, the SOI-induced $J_{\rm eff}$ states remain spectroscopically robust upon the substitution of the Ir ion with either the Rh or Ru ions. Further research efforts will elucidate the charge and spin transport subject to the large SOI.

ACKNOWLEDGMENTS

This research is granted by the Japan Society for the Promotion of Science (JSPS) through the "Funding Program for World-Leading Innovative R&D on Science and Technology (FIRST Program)," initiated by the Council for Science and Technology Policy (CSTP).

*jsl@gist.ac.kr

[1] K. I. Kugel and D. I. Khomskii, Sov. Phys. JETP **52**, 501 (1981).
[2] Y. Tokura and N. Nagaosa, Science **288**, 462 (2000).
[3] G. Cao, J. Bolivar, S. McCall, J. E. Crow, and R. P. Guertin, Phys. Rev. B **57**, R11039 (1998).
[4] B. J. Kim, j. Bolivar, S. McCall, J. E. Crow, and R. P. Guertin, Phys. Rev. Lett. **101**, 076402 (2008).
[5] B. J. Kim, H. Ohsumi, T. Komesu, S. Sakai, T. Morita, H. Takagi, and T. Arima, Science **323**, 1329 (2009).
[6] H. Watanabe, T. Shirakawa, and S. Yunoki, Phys. Rev. Lett. **105**, 216410 (2010).
[7] D. Pesin and L. Balents, Nat. Phys. **6**, 376 (2010).
[8] F. Wang and T. Senthil, Phys. Rev. Lett. **106**, 136402 (2011).
[9] O. B. Korneta, T. Qi, S. Chikara, S. Parkin, L. E. DeLong, P. Schlottmann, and G. Cao, Phys. Rev. B **82**, 115117 (2010).
[10] S. J. Moon, H. Jin, K. W. Kim, W. S. Choi, Y. S. Lee, J. Yu, G. Cao, A. Sumi, H. Funakubo, C. Bernhard, and T. W. Noh, Phys. Rev. Lett. **101**, 226402 (2008).
[11] M. A. Subramanian *et al.*, Physica C **235-l240**, 743 (1994).
[12] Y. Klein and I. Terasaki, J. Phys. Condens. Matter **20**, 295201 (2008).
[13] Y. Klein and I. Terasaki, J. Electron. Mater. **38**, 1331 (2009).
[14] C. Cosio-Castaneda, G. Tavizon, A. Baeza, P. de la Mora, and R. Escudero, J. Phys. Condens. Matter **19**, 446210 (2007).
[15] R. J. Cava, B. Batlogg, K. Kiyono, H. Takagi, J. J. Krajewski, W. F. Peck, L. W. Rupp, and C. H. Chen, Phys. Rev. B **49**, 11890 (1994).
[16] M. DeMarco, D. Graf, J. Rijssenbeck, R. J. Cava, D. Z. Wang, Y. Tu, Z. F. Ren, J. H. Wang, M. Haka, S. Toorongian, M. J. Leone, and M. J. Naughton, Phys. Rev. B **60**, 7570 (1999).
[17] K. S. Takahashi *et al.* (unpublished).
[18] J. S. Lee, M. Nakamura, D. Okuyama, R. Kumai, T. Arima, M. Kawasaki, and Y. Tokura, Phys. Rev. B **82**, 052406 (2010).
[19] Y. Krockenberger, M. Uchida, K. S. Takahashi, M. Nakamura, M. Kawasaki, and Y. Tokura, Appl. Phys. Lett. **97**, 082502 (2010).
[20] K. Okazaki, S. Sugai, Y. Muraoka, and Z. Hiroi, Phys. Rev. B **73**, 165116 (2006).
[21] S. J. Moon, H. Jin, W. S. Choi, J. S. Lee, S. S. A. Seo, J. Yu, G. Cao, T. W. Noh, and Y. S. Lee, Phys. Rev. B **80**, 195110 (2009).
[22] H. Kuriyama, J. Matsuno, S. Niitaka, M. Uchida, D. Hashizume, A. Nakao, K. Sugimoto, H. Ohsumi, M. Takata, and H. Takagi, Appl. Phys. Lett. **96**, 182103 (2010).
[23] S. Tajima, T. Ido, S. Ishibashi, T. Itoh, H. Eisaki, Y. Mizuo, T. Arima, H. Takagi, and S. Uchida, Phys. Rev. B **43**, 10496 (1991).
[24] L. Pintschovius, J. M. Bassat, P. Odier, F. Gervais, G. Chevrier, W. Reichardt, and F. Gompf, Phys. Rev. B **40**, 2229 (1989).
[25] S. J. Moon *et al.* (private communication).
[26] D. S. Fisher, G. Kotliar, and G. Moeller, Phys. Rev. B **52**, 17112 (1995).
[27] M. Imada, A. Fujimori, and Y. Tokura, Rev. Mod. Phys. **70**, 1039 (1998).
[28] S. Uchida, T. Ido, H. Takagi, T. Arima, Y. Tokura, and S. Tajima, Phys. Rev. B **43**, 7942 (1991).
[29] Y. Taguchi, Y. Tokura, T. Arima, and F. Inaba, Phys. Rev. B **48**, 511 (1993).
[30] M. J. Rozenberg, G. Kotliar, H. Kajueter, G. A. Thomas, D. H. Rapkine, J. M. Honig, and P. Metcalf, Phys. Rev. Lett. **75**, 105 (1995).
[31] M. K. Crawford, M. A. Subramanian, R. L. Harlow, J. A. Fernandez-Baca, Z. R. Wang, and D. C. Johnston, Phys. Rev. B **49**, 9198 (1994).
[32] $N_{\rm eff}$ can be obtained by integrating $\sigma_1(\omega)$ in a spectral range of the excitation of interest, e.g, between 0 and 0.4 eV for the inner-gap excitation, and the corresponding error bars are indicated for

$Sr_{2-y}La_yIrO_4$ and $Sr_2Ir_{1-x}Rh_xO_4$ in Fig. 5(b). For $Sr_2Ir_{1-x}Ru_xO_4$, the integration of $\sigma_1(\omega)$ with a fixed energy does not work since the inner-gap excitation becomes dominant with increasing x and the distinction among the excitation peaks is not clear. Therefore we increased the cutoff energy of the integration, e.g., 0.4 eV for $x = 0.02$ and 1.0 eV for $x = 0.26$, and used the values such obtained to account for the error bars.

[33] Y. Okimoto, T. Katsufuji, Y. Okada, T. Arima, and Y. Tokura, Phys. Rev. B **51**, 9581 (1995).

[34] T. Katsufuji, Y. Okimoto, and Y. Tokura, Phys. Rev. Lett. **75**, 3497 (1995).

[35] $N_{\rm eff}$ of the inner-gap excitation gradually increases upon the Rh substitution. Although this behavior is similarly observed upon the La substitution, which induces an electron doping, it should be understood differently, since the isoelectronic Rh substitution should preserve the band filling. Further investigation is desired to address in detail how the $J_{\rm eff} = 1/2$ state evolves with the reduction of the SOI strength.